

## TEXTURAL FEATURES OBSERVED UNDER POLARIZED LIGHT MICROSCOPY

F. HABIBY, Z. AHMAD, S. KHAN, A. UL HAQ AND A.Q. KHAN

*Matallurgy Division, Dr. A.Q. Khan Research Laboratories, Kahuta, P.O.Box 502, Rawalpindi, Pakistan*

(Received November 20, 1993 ; revised January 8, 1995)

Polarized microscopy can be used for semi-quantitative determination of crystal orientation. Due to difference in colour or grey contrast, polarized microscopy can be used to identify inclusions, and nucleating grains in the study of deformation and recrystallization processes. The usefulness of polarized microscopy has been demonstrated which shows microstructural features of various levels of grey colour contrast due to orientation differences. An X-ray Orientation Distribution Plot (ODF) is also presented to substantiate the inferences drawn on the basis of metallographic examination.

**Key Words.** Polarized light, Microstructural features, Electropolishing.

### Introduction

Polarized light microscopy exhibits different colours and shades which are produced due to optical anisotropy or surface topography. Thus, it is a powerful metallographic tool for the study of microstructural and textural features in deformed and recrystallized materials [1,2] for qualitative and semiquantitative assessment of the degree of preferred orientation [3].

In aluminum and aluminum alloys, an optically anisotropic surface layer can be produced by anodic oxidation to reveal orientation contrast of the substrate crystallites. The anodized surface produces different contrast under polarized light depending upon the orientation of the grains. This technique can be used to image different components of deformation texture, and to distinguish recrystallized grains from the deformed matrix. This technique can also be utilized to study the development of microstructural features as a results of various thermo-mechanical processes which is representative of the bulk specimen. This knowledge is particularly important in understanding textural features in the deformed and recrystallized materials.

This paper presents light polarized micrographs of aluminum and aluminum alloys which shows microstructural features of various levels of grey colour contrast due to orientation differences. X-ray ODF (orientation distribution function) plot is also presented to substantiate the inferences drawn on the basis of metallographic examinations.

### Materials and Methods

Pure aluminum, Al-0.4 wt% Si, and Al-0.8 wt% Si alloys were studied. Single crystals of Al-0.8 wt% Si were also grown by modified Bridgeman technique. A heat-treatment [2] was used to produce predominantly equiaxed Si precipitates of 0.5 to 6  $\mu\text{m}$  diameter to study the effect of second phase particles on the deformed and recrystallized structure. Samples for microscopy were first mechanically polished, using 800 and

1200 sic grit paper and 3  $\mu\text{m}$  diamond paste. A solution of 30% nitric acid in methanol, at a potential of 20 V and at a temperature of  $-25^{\circ}\text{C}$  was used for electro-polishing. Finally, Barker's reagent (46 cc  $\text{HBF}_4$  + 7g boric acid + 970 cc  $\text{H}_2\text{O}$ ) was used for anodizing. A suitable anodic film was usually achieved after 2 to 3 mins at a potential of 20 V with current density of 0.5  $\text{A}/\text{cm}^2$ .

### Result and Discussion

**Microstructural features.** Microstructural features due to orientation contrast are presented in Figs. 1-6 along with an Orientation Distribution Function (ODF) plot (Figs. 6b, 7 and 8) to substantiate the inferences drawn on the basis of micrographs obtained by light polarized microscopy. Figure 1 portrays the potentials of using light polarized microscopy over light optical microscopy in examining FCC materials which are optically isotropic. Featureless microstructure is observed in as polished condition (Fig. 1a) in Al-0.8 wt% Si single crystal with fine distribution of 0.5-0.7  $\mu\text{m}$  Si particles after 50% uniaxial compression. Same specimen after anodizing reveals orientation contrast due to deformation bands (Fig. 1b).

Poly-crystalline pure aluminum is fully recrystallized to obtain a microstructure which is depicted in Fig. 2a. Microstructure shows various levels of grey shades (ranging from black to white) from grain to grain which reflects the magnitude of misorientation among them. Grains marked as 1 (white) and 2 (black) represent relatively large misorientation as compared to grain 2 (black) and grain 3 (grey). Same specimen after 30% cold rolling shows regions of misorientation or deformation bands within grains (arrows). Deformation bands which are an essential part of a deformed structure are observed to be influenced by non-deformable second phase particles [2]. Figure 3 shows deformation bands of very different morphology in Al-0.8 wt.% Si single crystal compared with those observed in Fig. 1a in crystal of identical

orientation but different particle size.

Nucleation of recrystallization can also be observed conveniently by polarized microscopy, the evidence of which is not revealed under simple optical microscopy. Figure 5 shows nucleation of new grains by strain induced boundary migration (SIMB) in which a sub cell (or subgrain) of one grain adjacent to a pre-existing high angle grain boundary grows by migration of that boundary into the neighbouring grain. Nu-

cleation of many new grains can also be seen at the prior grain boundaries in heavily deformed material (Fig. 5b).

Nucleation of recrystallization in particle-containing materials is observed by a mechanism called particle stimulated nucleation (PSN) if the particles are of a critical size [4,5]. Figure 6a depicts a recrystallized microstructure of Al-0.4 wt% Si alloy in which a bimodal distribution of Si particles are achieved by heat-treatment. At the grain boundary the particle

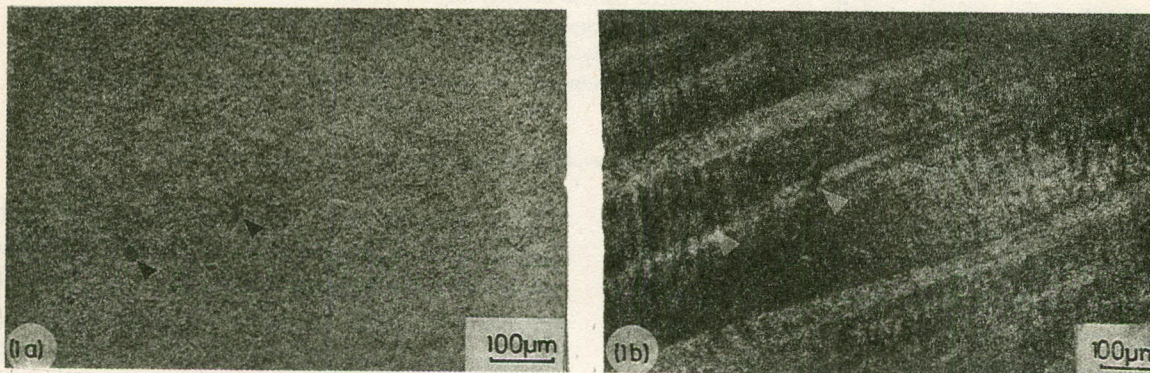


Fig. 1. Featureless microstructure observed in as polished condition in particle-containing Al-Si single crystal (a). Same specimen after anodizing reveals deformation bands (b) Arrows show inclusions which serve as reference marks.

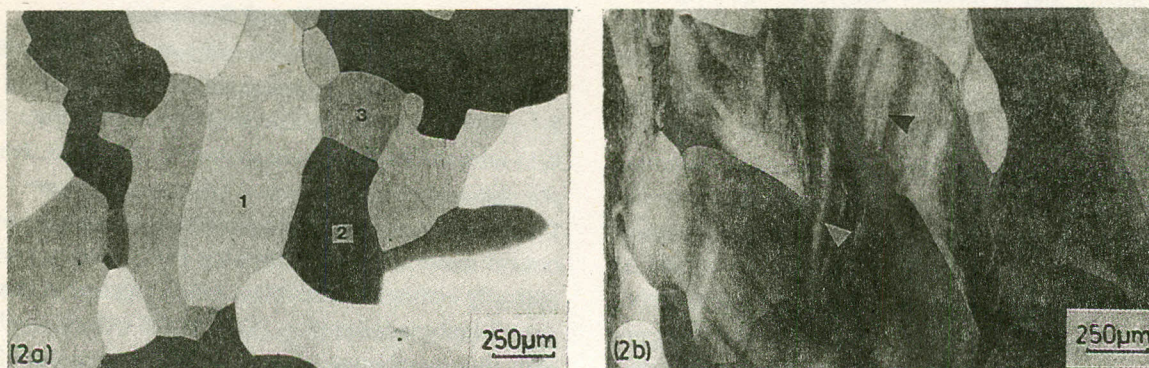


Fig. 2. Polycrystalline pure aluminium in fully recrystallized state (a). Same sample after 30% cold rolling showing deformation bands (arrows) within grains (b).

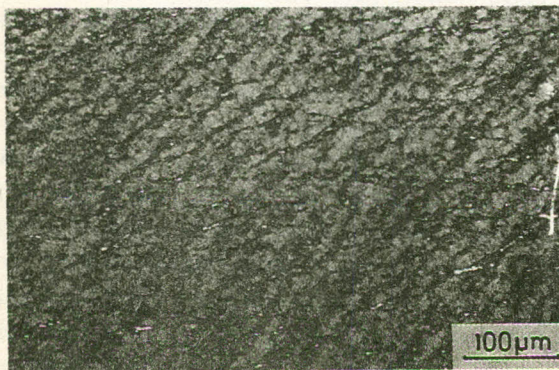


Fig. 3. Single crystal of Al-0.8 wt% Si with 1.5-5 µm Si particles showing deformed microstructure after 50% uniaxial compression.

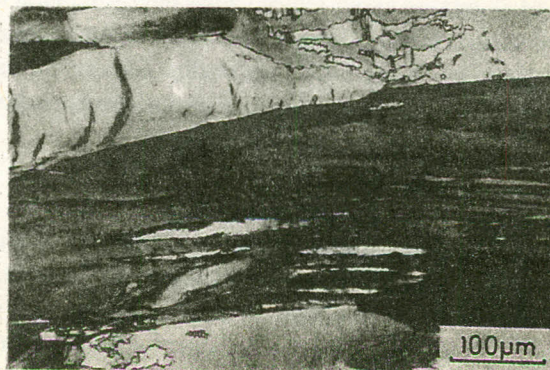


Fig. 4. Polycrystalline pure aluminium showing deformed structure after 50% hot rolling.

size is significantly larger (6  $\mu\text{m}$ ) as compared to the interior of the grain (0.6  $\mu\text{m}$ ). When this alloy is cold rolled and subsequently recrystallized particle stimulated nucleation is observed at the prior grain boundary resulting in equiaxed grains and elongated new grains in the interior of the old

deformed grain. Equiaxed and elongated grains may be expected to have a different crystallographic texture. Orientation Distribution Function (ODF) of same specimen ( $\Phi = 45^\circ$  section) presented in Fig 6b confirms presence of Goss  $[112]$   $\langle 110 \rangle$ , Brass  $\{011\} \langle 211 \rangle$ , and Cube  $\{001\} \langle 100 \rangle$  texture

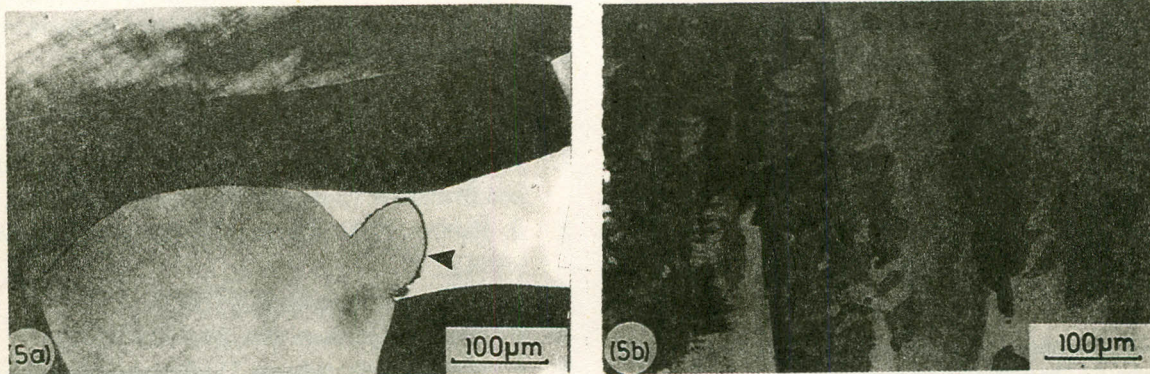


Fig. 5. Recrystallization by strain induced boundary migration (SIBM) in pure aluminium cold rolled 30% and annealed at 250°C (a). Nucleation of new grains at the prior grain boundaries in a similar specimen at 70% reduction and annealed at 250°C (b).

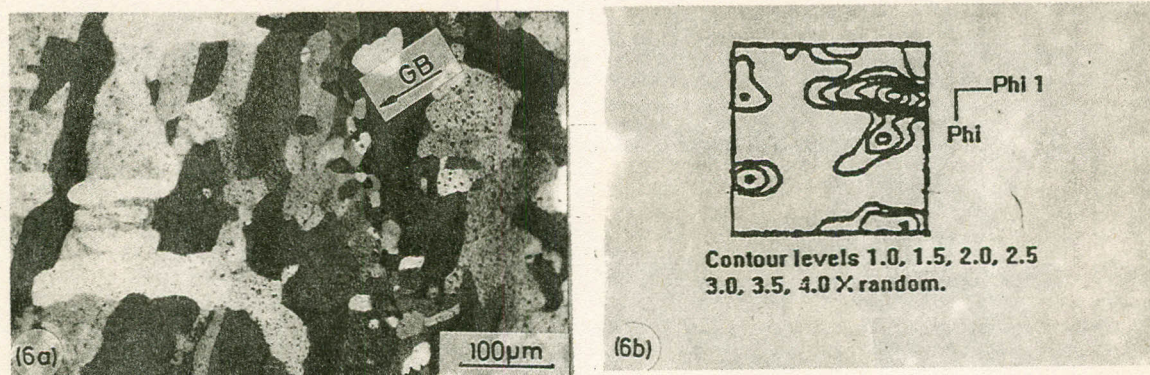
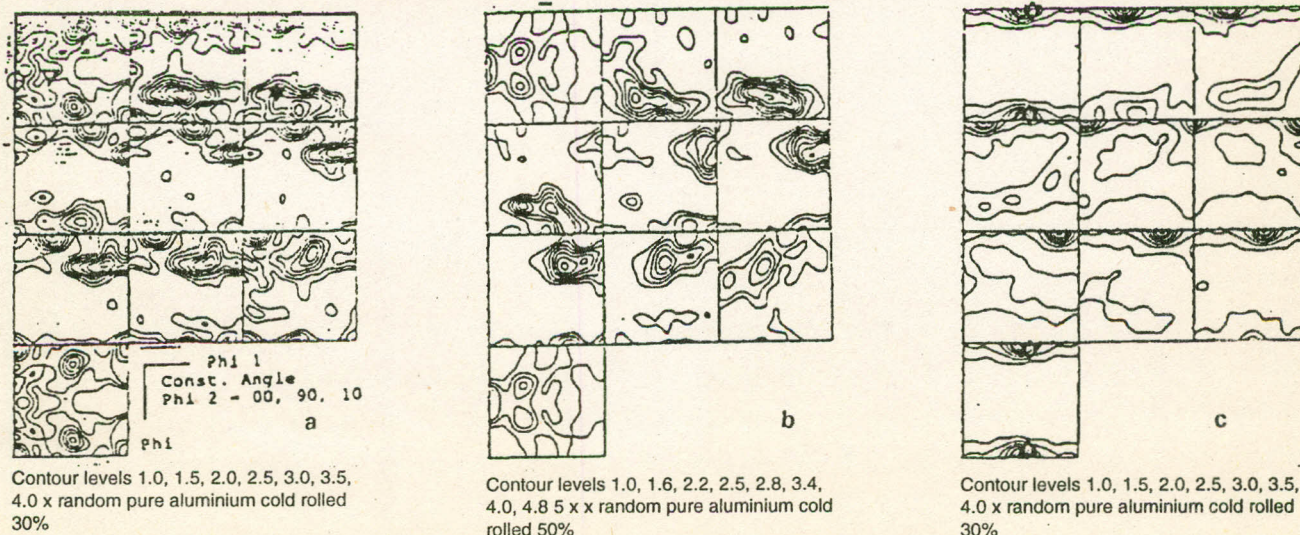


Fig.6. Particle stimulated nucleation at the grain boundary resulting in equiaxed grains. Elongated recrystallized grains are seen within the previously deformed grains (a). Orientation distribution function (ODF) of same specimen ( $\Phi = 55^\circ$  section) confirms presence of various texture components (b).



Contour levels 1.0, 1.5, 2.0, 2.5, 3.0, 3.5, 4.0 x random pure aluminium cold rolled 30%

Contour levels 1.0, 1.6, 2.2, 2.5, 2.8, 3.4, 4.0, 4.8 5 x x random pure aluminium cold rolled 50%

Contour levels 1.0, 1.5, 2.0, 2.5, 3.0, 3.5, 4.0 x random pure aluminium cold rolled 30%

Fig.7. Orientation distribution function plots of pure Al at different strain rate showing different development of texture.

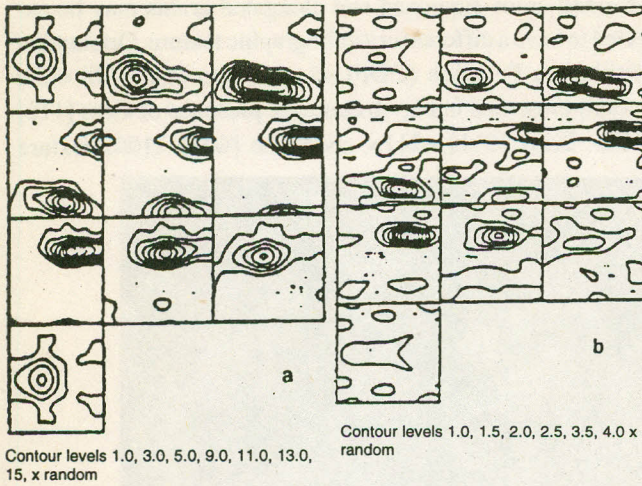


Fig. 8. Orientation Distribution Function plots of Al-0.4 wt%Si (a) and Al-0.8 wt% Si alloy (b). The texture in (b) is much weaker as compared to one observed in (a).

components. Figure 7 presents ODF of pure Al as a function of cold rolling. These ODF confirm the results of Fig. 6b. Figure 8 compares the ODF of Al-0.4 wt% Si (Fig. 8a) and Al-0.8 wt% Si (Fig 8b). This indicates that texture in samples of Al-0.8 wt% Si is much weaker as compared to the samples of Al-0.4 wt% Si. Thus it may be concluded that increase in Si particles lead to the softening of the texture.

#### References

1. H. Morrogh, *Polarized Light in Metallography* Ed. Conn and Bradshaw, (Butterworths, London 1952), pp. 88.
2. F. Habiby, Ph.D. Thesis, University of London, U.K (1991).
3. H. Tas, *Metallography*, **6**, 8 (1973).
4. F.J. Humphreys, *Acta Met*, **25**, 1323 (1977).
5. F. Habiby, F.J. Humphreys, *Textures and Microstructures*, **20**, 723 (1993).